The British Journal of Radiology, 85 (2012), e1256–e1262

The influence of MRI scan position on image registration accuracy, target delineation and calculated dose in prostatic radiotherapy

[1]S HANVEY, MSc, [2]A H SADOZYE, FRCR, FRCP, [1]M McJURY, PhD, [1]M GLEGG, MSc and [1]J FOSTER, PhD

[1]*Department of Clinical Physics and Bioengineering, Beatson West of Scotland Cancer Centre, Glasgow, UK, and*
[2]*Department of Clinical Oncology, Beatson West of Scotland Cancer Centre, Glasgow, UK*

Objective: To investigate the necessity of performing MRI in the radiotherapy position when using MRI for prostatic radiotherapy.
Methods: 20 prostate patients received a CT, diagnostic MRI and an MRI scan in the radiotherapy position. The quality of registration between CT and MRI was compared between the two MRI set-ups. The prostate and seminal vesicles were contoured using all scans and intensity modulated radiotherapy (IMRT) plans were generated. Changes in the target volume and IMRT plans were investigated. Two-tailed paired Student's *t*-tests determined the statistical significance.
Results: There was a decrease in the mean distance from the centre of the bony anatomy between CT and MRI (from 3.9 to 1.9 mm, p-value<0.0001) when the MRI scan was acquired in the radiotherapy position. Assuming that registering CT with an MRI scan in the radiotherapy position is the gold standard for delineating the prostate and seminal vesicles, using a planning target volume delineated on the CT with a diagnostic MRI scan viewed separately, resulted in a mean conformation number of 0.80 instead of the expected 0.98 ($p<0.0001$).
Conclusion: By registering CT with an MRI scan in the radiotherapy position, there is a statistically significant improvement in the registration and IMRT quality.
Advances in knowledge: To achieve an acceptable registration and IMRT quality in prostatic radiotherapy, neither CT with a separate diagnostic MRI nor CT registered to a diagnostic MRI will suffice. Instead, a CT registered with an MRI in the radiotherapy position should be used.

Received 13 July 2012
Accepted 25 July 2012

DOI: 10.1259/bjr/26802977

It is of the utmost importance that the radiotherapy (RT) planning process accurately defines the gross tumour volume (GTV) and organs at risk for successful patient management. Many centres routinely register MRI to CT data sets to take advantage of the superior soft-tissue contrast of MRI and the electron density information from CT.

The use of dose escalation techniques, such as intensity modulated radiotherapy (IMRT), enables the delivery of high radiation dose to irregular target volumes with increased sparing of healthy tissue over conventional static field RT. Additionally, the more conformal delivery of radiation dose places greater importance on the localisation of the GTV, given that IMRT can generate high doses with steep dose gradients.

Typically, external beam RT planning uses CT axial images to define the tumour volume. Because CT offers excellent visualisation of bony anatomy and electron density information, it has largely been the favoured modality for RT planning. However, CT is poor at distinguishing between structures with similar electron densities. An example of this is the prostate and seminal vesicles, where it is difficult to distinguish the extent of the prostate from the surrounding soft tissue.

The improved soft-tissue contrast of MRI enables more accurate localisation of adjacent critical soft-tissue over CT [1]. MRI has reduced interference from metal implants such as prosthetic hips [2] and gold seed implants and therefore has the potential to provide improved target volume delineation over CT. Changes in anatomical and tumour definition as a result of using MRI data compared with CT have been reported for prostate [2–7], head and neck [8–11] and brain cancer [12, 13] patients.

Registration of MRI to CT is an effective method of gaining both the improved target definition of MRI and the geometric accuracy and electron density of CT. However, although MRI provides improved soft-tissue contrast, there are several difficulties with integrating MRI into the RT planning process. MRI is known to suffer from geometric distortion owing to the non-linearity of the imaging gradients over large fields of view [14]. Today, most vendors provide in-plane distortion correction to deal with this [5]. Owing to the lengthy scan times of MRI, motion artefacts can diminish the image quality and alter the accuracy of target localisation. Magnetic susceptibility should also be considered, as this can affect the homogeneity of the main magnetic field, leading to further distortion [15, 16]. It is also important that patients are positioned the same way in

Address correspondence to: Dr Scott Hanvey, Radiotherapy Physics, Beatson West of Scotland Cancer Centre, 1053 Great Western Road, Glasgow G12 0YN, UK. E-mail: scott.hanvey@ggc.scot.nhs.uk
The authors would like to acknowledge financial support from the NHS Learning and Education and The Beatson Oncology Centre Fund.

MRI as they are for CT. Changes in patient position in MRI can lead to misalignments when registering with CT. The difference in the shape of the MRI table from the CT table is one reason for the misalignment in registration.

There have been a number of studies published investigating rigid registration accuracy [17–20]. Moore et al [17] assessed the registration accuracy of their treatment planning system by outlining structures on a registered phantom. Using the position, area and perimeter of each structure and with a coefficient of agreement analysis, the accuracy of the image registration algorithm was determined. Another group [18] used anatomical landmarks to determine the registration accuracy of CT and MRI data sets.

The aim of this study was to determine how different patient positions in MRI affected the registration quality with CT. A further goal of this research was to examine the changes in the target volume and how this affects RT planning. It was the overall intention of this article to determine if it was necessary to obtain an MRI scan in the RT position for RT planning or whether a diagnostic MRI scan would suffice.

An attempt was made to register the CT and MRI data sets using the prostate seeds as registration points to then transform the MRI coordinate system to the CT. Our treatment planning system (Eclipse™, Varian Medical Systems, Inc., Palo Alto, CA, v. 8.6.15) could not perform the registration because of the close proximity of the seeds to one another. Changing the volume of interest to include only the prostate so that the registration was performed using the pixel data within the volume of interest resulted in poor registration. There was also no change to the registration results by prioritising the prostate volume. Although deformable registration is available for Eclipse, it does not allow multimodality registration. As with most UK RT centres, deformable CT–MRI registration is not used clinically at our centre and so was not investigated.

Although it could be anticipated that imaging the patient in the same orientation as they receive their treatment would result in an improvement in the registration, many RT centres neither register the CT with MRI nor ensure the MRI positioning is consistent with treatment. Furthermore, the authors were unable to find a publication which rigorously tests the theory presented in this study. It is anticipated that by addressing the problems related to changes in the tumour volume, registration and, importantly, the subsequent effect on prostatic RT, this will facilitate an adjustment in current practice.

Methods

Patient group and study overview

20 prostate cancer patients (age 56–75 years) due to undergo RT were selected for the study. This investigation was approved by the local ethics committee. Informed consent was obtained from all patients before entering into this study. The patients received a CT planning scan, an MRI scan in the typical diagnostic position, MRI_D, and an MRI scan in the RT position, MRI_{RT}, during the same scan session. Both MRI scans were registered separately with CT, as shown in Figure 1. Delineations of bony and soft-tissue volumes were made on the CT with the MRI_D viewed on a separate console (CT_S), as is the current practice at our centre. Volumes of bony and soft-tissue structures were also delineated with the CT registered to the MRI_D (CT–MRI_D) and the CT registered to the MRI_{RT} (CT–MRI_{RT}).

CT scanning protocol

Patients were scanned on a GE LightSpeed RT 16 CT scanner (GE Medical Systems, Milwaukee, WI) using the current clinical scanning protocol. All patients received three gold seed implants to the prostate for positioning adjustment at treatment. Patients were asked to empty their bladder before being given 200 ml of water 30 min before their scan. To immobilise the patients, a knee support and head rest were used. Using a LAP laser positioning system (DORADO 3; LAP Laser, Lüneburg, Germany) the patients were aligned with the laser, and lateral and anterior markers were placed on the patient. Following the scout scan, tattoos were located 1 cm

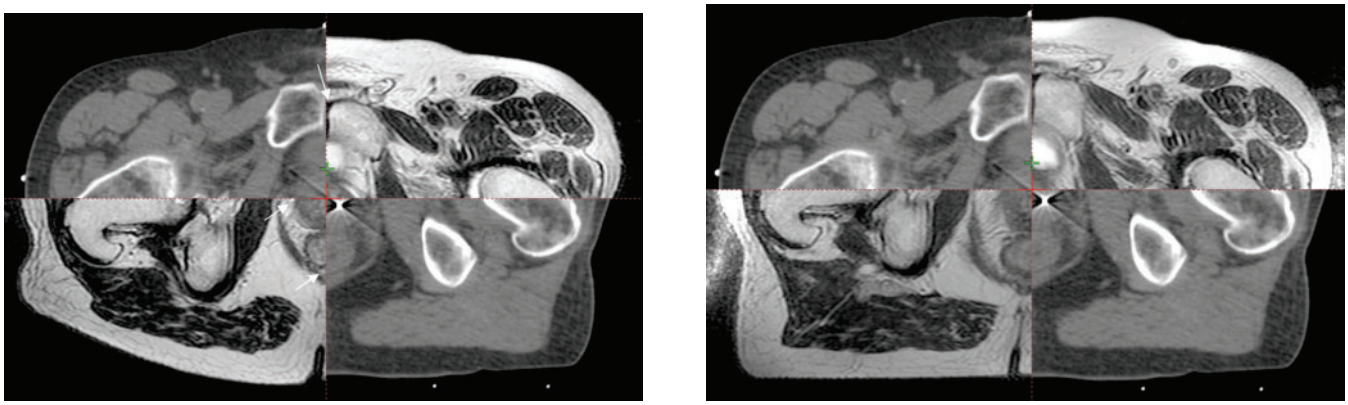

(a) (b)

Figure 1. Split view showing the registration of (a) the CT and MRI_D and (b) the CT and MRI_{RT} data sets. White arrows on image (a) indicate errors in registration which can be seen to be corrected on (b). MRI_D, diagnostic MRI scan; MRI_{RT}, MRI scan in the radiotherapy position.

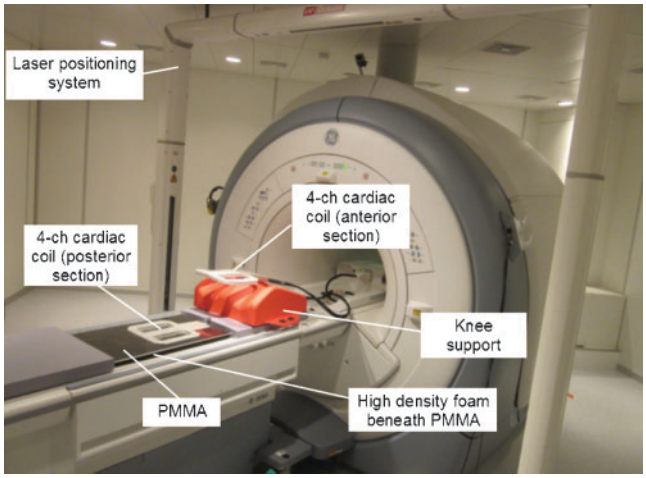

Figure 2. MRI_{RT} flat table set up. MRI_{RT}, MRI scan in the radiotherapy position; 4-ch, four-channel; PMMA, polymethyl methacrylate.

below the superior border of the symphysis pubis and 1 cm anterior to half of the patient's anteroposterior separation. A scan extent of inferior superoinferior joints to 3 cm below the inferior pubic ramus was used. A helical scan was acquired with a detector configuration of 16×1.25 mm, pitch 0.938 and speed 18.75 mm per rotation with a slice thickness and interval of 2.5 mm.

MRI scanning protocol

Patients received their MRI scans without contrast, in accordance with the clinical protocol, on a GE Signa HDxt 1.5 T MRI scanner (GE Medical Systems). Weekly geometric linearity and distortion measurements are conducted on this scanner. It was found that the linearity error did not exceed 0.3 mm, and the distortion coefficient of variation was no more than 0.3% over the past 12 months. In addition, monthly uniformity and slice position measurements are performed. The percentage image uniformity measurements were found to be at worst 96.0%, and the largest average slice position error was 0.6 mm for a given month over the previous 12 months. These results were within the tolerances defined in the Institute of Physics in Engineering and Medicine Report 80 and the American Association of Physicists in Medicine Report 100 [21, 22].

The patients were scanned in two different positions. For the MRI_{RT} scan, patients were positioned on a customised polymethyl methacrylate (PMMA) sheet, to simulate the treatment couch, with a four-channel flexible surface cardiac coil beneath the PMMA positioned posterior to the prostate and another positioned on the anterior surface of the patient, as shown in Figure 2. The posterior section of the four-channel cardiac coil was held flat against the underside of the PMMA using high-density foam, to maximise the signal-to-noise ratio (SNR). The same knee rest immobilisation and a similar bladder preparation were used for the MRI_{RT} and CT scan, except there was a delay of only 15 min after drinking the required volume of water for the MRI scans to take into account the longer scan times. Using the permanent skin markers the patients were firstly positioned with the markers at the centre of the four-channel imaging coil to maximise the signal at the prostate. Patients were then aligned in the same way as their CT using the markers and an LAP laser positioning device, and this became the isocentre plane and central slice. A similar scan extent was used as the CT scan. The imaging parameters used for the T_1 and T_2 weighted scans are shown in Table 1.

The patient was then removed from the table and a standard diagnostic scan was performed using a curved couch and eight-channel cardiac coil during the same scan session. This scan was repeated in the same way as the flat table MRI scan except that the patients were not aligned with the LAP laser positioning device, but were positioned in the magnet as for a typical diagnostic MRI scan of the pelvis. The eight-channel cardiac coil was not used for the MRI_{RT} scan because this coil is curved and rigid, so there would have been a greater distance between the patient and the posterior section of the coil than with the four-channel cardiac coil. This would have resulted in a reduced SNR of approximately 14% [23] and could potentially have prevented very large patients participating in the study, owing to the restrictions of the magnet bore size.

Image registration

The CT data set was registered with the MRI_{RT} and MRI_D T_1 and T_2 weighted scans using Eclipse. This software performed a fully automatic, mutual information-based rigid registration. The entire scanned pelvis was used for the registration to provide as much information for the registration algorithm as possible. A fully automatic registration was used to keep user interaction to a minimum.

To assess the registration accuracy a trained expert outlined three rigid volumes on the CT and MRI T_1 weighted data sets. The volumes delineated were the symphysis pubis and three transverse sections of the left and right femoral heads. The transverse sections chosen for the femoral heads were at the most inferior level of the ischial tuberosity, the most inferior aspect of the symphysis pubis and the transverse section above the most proximal slice in which the femoral neck is in continuity with the femoral head. This bony anatomy

Table 1. MRI parameters

Scan type	FOV (mm)	Slice thickness (mm)	Spacing (mm)	TE (ms)	TR (ms)	Matrix size	ETL	Scan duration (min)
2D driven-equilibrium FSE (T_2 weighted)	480	2.5	0	93.9	2520	512×256	17	5:19
3D FSPGR (T_1 weighted)	480	2.5	0	2.2	4.5	512×384	N/A	6:11

2D, two dimensional; 3D, three dimensional; FOV, field of view; TE, echo time; TR, repetition time; ETL, echo train length; FSE, fast spin echo; FSPGR, fast spoiled gradient echo.

was delineated firstly, as is standard practice, on the CT_S and then repeated on the registered image sets CT–MRI_D and CT–MRI_{RT} for each patient. The centre of each of these volumes was determined and the distance between the volume centre on MRI and CT was measured.

Gross tumour volume delineation

A trained consultant clinical oncologist delineated two volumes for all patients; the prostate and the prostate plus seminal vesicles. Delineation of the two volumes was firstly performed on the CT_S. Next, the clinician contoured the volumes on the registered CT–MRI_D data sets and then finally re-outlined using the CT–MRI_{RT}. When delineating on the registered image sets, the clinician was able to view both the CT and the MRI information at the same time. The clinician used the T_2 weighted MRI data sets for contouring the prostate and seminal vesicles. There was a period of at least a week between delineations of the same patient using a different set-up and the oncologist was blinded to previous delineations. These prostate volumes delineated using the three set-ups were later expanded to planning target volumes (PTVs) for IMRT planning.

Data analysis

The quality of registration was assessed in two ways: by measuring the spatial overlap of the CT and MRI volumes and by measuring the distance from the centre of the volumes drawn in CT to those delineated in MRI.

The spatial overlap for the CT and MRI volumes was assessed by calculating the volume overlap index (VOI) for each volume. The VOI is given by:

$$\mathrm{VOI} = \frac{\text{Volume of intersection between CT and MRI}}{(\mathrm{CT} + \mathrm{MRI\ volume})/2} \quad (1)$$

such that the value of the VOI ranges from 0, which indicates no spatial overlap between the CT and MRI volumes, to 1, which is complete overlap [24]. As volumes outlined on CT and MRI may differ, even with perfect registration, a VOI of 1 may not be achieved in practice. However, comparisons of VOIs for the MRI volumes with different patient set-up and registration quality will show changes in VOI that are dependent on these differences.

To determine the effect changes in tumour volumes have on RT planning, IMRT plans were generated for each patient. For each patient, three IMRT plans were calculated by optimising for three PTVs generated from the prostate volumes delineated using the three set-ups described in the last section. In accordance with the Conventional or Hypofractionated High Dose Intensity Modulated Radiotherapy for Prostate Cancer (CHHiP) trial [25] the PTV is defined as the prostate plus a 5-mm margin in all directions, except in the posterior direction where there is no additional margin, and excludes the rectal volume.

The IMRT plans were calculated using the CHHiP trial dose constraints and the pencil beam convolution algorithm in Eclipse (Varian Medical Systems, Inc) v. 8.2.23. With this set of PTVs, we have taken each PTV in turn and assumed for analysis that it is the volume for clinical planning, and optimised the plan for this volume. However, if owing to differences in image registration and patient set-up one of the other PTVs is in fact the ''true'' volume to be targeted, for each clinical plan we have then also analysed the dosimetry of the other two PTVs to investigate the doses which would have been delivered to the true target from our plan. For example, our current practice is to generate a clinical plan based on set-up CT_S where the PTV is contoured on the CT images while viewing MRI data on a separate workstation. The PTV based on CT_S is optimised in planning, but with improved image registration; PTVs based on the other two set-ups may be the true volume, and so doses delivered to these non-optimised volumes are investigated.

For each plan, a conformation number (CN) was calculated for each of the three PTVs. The CN indicates the extent to which the target volume is being irradiated and healthy tissue is being spared, as shown in Equation (2). The first fraction of the equation relates to the quality of the target coverage while the second fraction is an indicator of healthy tissue sparing. The CN varies from 0 to 1, where 1 is the ideal value and the target is covered completely with total sparing of the surrounding healthy tissue [26]. With the CN it is possible to establish the quality of the RT plan for the PTV in each set-up. The PTV for which the plan was optimised would be expected to have a high value of CN, whereas the CN for the other two non-optimised PTVs will reflect the impact of registration differences on the planning doses. Assuming that the PTV based on the CT–MRI_{RT} is the gold standard, it is possible to determine the extent to which the CT_S and CT–MRI_D PTVs achieve a similar IMRT quality.

The CN is defined according to the following equation [26]:

$$\mathrm{CN} = \frac{\mathrm{TV_{RI}}}{\mathrm{V_{PTV}}} \times \frac{\mathrm{TV_{RI}}}{\mathrm{V_{RI}}} \quad (2)$$

where TV_{RI} is the target volume covered by the reference isodose, V_{PTV} is the volume of the PTV and V_{RI} is the volume of the reference isodose. The reference isodose volume is defined as the volume receiving the therapeutic prescribed dose.

Two-tailed paired Student's *t*-tests were performed to examine the statistical significance of the differences of the registration quality and dosimetric indices. The null hypothesis was rejected when $p<0.05$.

Results

The mean prostate and prostate plus seminal vesicles volumes were found to be significantly larger when the clinician contoured on CT_S rather than on CT–MRI_D or the CT–MRI_{RT}, as shown in Table 2. The *p*-values in Table 2 refer to the differences in the prostate and prostate plus seminal vesicles volumes delineated on the CT_S to those drawn using the CT–MRI_D or CT–MRI_{RT}. For these volumes there was shown to be an improvement in the

Table 2. Changes in mean volume and volume overlap index (VOI) of the prostate and prostate plus seminal vesicles in the different set-ups. The *p*-values refer to the differences in the prostate and prostate plus seminal vesicles volumes delineated on the CT_S to those drawn using the CT–MRI_D or CT–MRI_{RT}

		CT–MRI_D		CT–MRI_{RT}	
Structure	Mean CT_S volume ± SD (cm^3)	Mean volume ± SD in cm^3 (*p*-value)	Mean VOI	Mean volume ± SD in cm^3 (*p*-value)	Mean VOI (cm^3)
Prostate	36.3±10.8	32.0±11.1 (0.001)	0.70	31.4±11.0 (0.001)	0.74
Prostate and seminal vesicles	45.9±12.0	41.2±12.9 (0.001)	0.64	40.3±12.5 (0.002)	0.69

CT_S, CT with the diagnostic MRI scan viewed on a separate console; CT–MRI_D, CT registered with the diagnostic MRI scan; CT–MRI_{RT}, CT registered with the MRI scan in the radiotherapy position; SD, standard deviation.

mean VOI using the CT–MRI_{RT} rather than the CT–MRI_D (Table 2). A significant difference was found in the VOI between the prostate volumes delineated on the CT_S and CT–MRI_D and between the CT_S and the CT–MRI_{RT} ($p=0.045$) but not for the prostate plus seminal vesicles volumes ($p=0.058$). The mean VOI for the bony landmarks also demonstrated an improvement for the CT–MRI_{RT} over the CT–MRI_D data sets, as shown in Table 3. Combining the VOI results for the bony anatomy by averaging the data for the left and right femoral heads and symphysis pubis gave a mean VOI of 0.67 for the CT–MRI_D, compared with 0.74 for the CT–MRI_{RT} ($p=0.046$).

Qualitatively, it is evident from Figure 1 that the MRI_{RT} offers improved registration with CT over the MRI_D. A registration mismatch is indicated by white arrows in the CT–MRI_D shown in Figure 1a. This was measured quantitatively as a reduction in the mean distance from the centre of the CT to the MRI_{RT} volumes to that of the CT to MRI_D volumes (Table 4). A statistically significant improvement was found in the registration accuracy of the bony anatomy with CT to MRI_{RT} over the MRI_D data sets ($p<0.0001$). In Table 4 the results are presented with their standard deviations. It can be seen that the bony anatomy results show a reduction in the standard deviation values for the CT data set registered to the MRI_{RT} rather than the MRI_D. This is due to the use of patient positioning lasers to set-up the patients for their MRI_{RT} scan. The lasers enabled the patients to be positioned for their MRI_{RT} scan more closely to their CT set-up position and thereby resulted in a reduction in the set-up error, whereas for their MRI_D scan the patients were not aligned with the positioning lasers and so were unlikely to be scanned in the same plane as their CT scan.

Additionally, there was a decrease in the mean distance from the centre of the prostate and prostate plus seminal vesicles volumes delineated on the CT_S to the CT–MRI_{RT} compared with the volumes drawn on the CT–MRI_D (Table 4). There was a statistically significant difference between the distance from the centre of the prostate and prostate plus seminal vesicles volumes delineated on the CT_S and the CT–MRI_D to the CT_S and the CT–MRI_{RT} ($p=0.021$).

The CT_S, CT–MRI_D and CT–MRI_{RT} conformation numbers for the PTV are shown in Table 5. These results indicate that when the RT plan has been optimised for that PTV an average CN of 0.98 can be achieved.

If it is assumed that the CT–MRI_{RT} is the gold standard for delineating the prostate and seminal vesicles then the current method using the CT_S results in a mean CN of 0.80 instead of the expected 0.98 ($p<0.0001$) for the PTV. If instead the CT–MRI_D volumes are used, this leads to a mean CN of 0.85 instead of the expected 0.99 ($p=0.0001$) for the PTV, taking CT–MRI_{RT} as the gold standard. All PTV optimisation combinations were assessed but are not recorded because they are not clinically relevant.

Table 3. Changes in mean volume overlap index (VOI) of the bony landmarks for the two registration set-ups

Structure	CT–MRI_D mean VOI	CT–MRI_{RT} mean VOI
Left femoral head	0.77	0.85
Right femoral head	0.72	0.81
Symphysis pubis	0.52	0.56

CT–MRI_D, CT registered with the diagnostic MRI scan; CT–MRI_{RT}, CT registered with the MRI scan in the radiotherapy position.

Discussion

The importance of registering the MRI to the CT data set is demonstrated by the statistically significant difference between the prostate and prostate plus seminal vesicle volumes when the clinician contoured on the CT_S rather than the registered data sets. This is due to the difficulty in determining the extent of the prostate and seminal vesicles in CT because of the similarity in Hounsfield numbers with the surrounding tissue, which results in a lack of contrast.

The changes in target volume in this study are in agreement with several other studies [2–7], which have demonstrated that outlining prostate and seminal vesicles using MRI results in smaller volumes and anatomically more accurate delineation. One study [7] has shown that outlining with MRI results in a smaller volume of

Table 4. Quality of registration results, where the mean error is the distance from the centre of the CT structures to the centre of the MRI structures

Structure	CT to MRI_D mean (mm)	CT to MRI_{RT} mean (mm)
Left femoral head	3.0±2.2	2.0±1.6
Right femoral head	3.4±1.8	1.8±1.2
Symphysis pubis	5.2±3.0	1.8±1.1
Prostate	5.0±2.5	3.6±2.2
Prostate and seminal vesicles	5.2±2.3	4.1±2.6

MRI_D, diagnostic MRI scan; MRI_{RT}, MRI scan in the radiotherapy position; SD, standard deviation.

Table 5. Mean CN for CT_S, $CT–MRI_D$ and $CT–MRI_{RT}$ when optimised for PTV in the three set-ups

PTV for which the IMRT plan was optimised	PTV under examination	Mean CN ± SD
CT_S	CT_S	0.98 ± 0.03
$CT–MR_D$	$CT–MR_D$	0.99 ± 0.01
$CT–MR_{RT}$	$CT–MR_{RT}$	0.98 ± 0.06
CT_S	$CT–MR_{RT}$	0.80 ± 0.11
$CT–MR_D$	$CT–MR_{RT}$	0.85 ± 0.13

PTV, planning target volume; IMRT, intensity modulated radiotherapy; CT_S, CT with the diagnostic MRI scan viewed on a separate console; $CT–MRI_D$, CT registered with the diagnostic MRI scan; $CT–MRI_{RT}$, CT registered with the MRI scan in the radiotherapy position; CN, conformation number; SD, standard deviation.

rectal wall being included, potentially leading to a reduced risk of late toxicity.

As mentioned previously, a VOI of 1 may not be attained because of the differences in the volumes delineated on MRI and CT. In this study the relative changes in the VOI were assessed. An improvement in the mean VOI of the prostate and prostate plus seminal vesicle was evident for $CT–MRI_{RT}$ over $CT–MRI_D$ images. This was seen to be significant for the prostate but not the prostate plus seminal vesicle volumes, owing to the difficulty in delineating the seminal vesicles, particularly on CT. These data indicate that the prostate volume is more accurately matched to the CT for the MRI_{RT} than the MRI_D. This was confirmed by a reduction in the average distance between the centre of the prostate and prostate plus seminal vesicles volumes delineated on CT_S to that on $CT–MRI_{RT}$ rather than $CT–MRI_D$. The improved VOI and reduced error between CT and MRI_{RT} for the prostate and seminal vesicles offers the clinician greater confidence in the use of MRI for radiotherapy planning.

The quality of registration to CT improved using the MRI_{RT} instead of the MRI_D images. This was demonstrated by a statistically significant reduction in error of the rigid bony landmarks from CT to the MRI_{RT} to that drawn on the CT and MRI_D data sets. This was further confirmed by an improvement in the VOI of the bony landmarks when using the CT and MRI_{RT} rather than the CT and MRI_D images. It can be seen that the bony anatomy results show a reduction in the standard deviation values for the CT data set registered to the MRI_{RT} rather than the MRI_D. While the standard deviation values for the prostate were also reduced with the $CT–MRI_{RT}$, the prostate plus seminal vesicle volumes slightly increased. This again highlights the challenges associated with delineating the seminal vesicles. Accurate target localisation becomes more important as RT planning moves towards dose escalation and dose painting techniques with high-dose gradients.

From the results it has been verified that there is a statistically significant improvement in the quality of IMRT plans when registering CT with MRI_{RT} rather than using CT_S or $CT–MRI_D$. The improvement in the quality of IMRT planning using the $CT–MRI_{RT}$ demonstrates that it would be suboptimal to rely on the CT_S or $CT–MRI_D$ for prostatic RT planning.

Conclusion

This study has shown that when MRI scans are performed in the RT position for prostatic RT planning significant improvements in the quality of MR registration and IMRT can be achieved.

Acknowledgments

The authors would like to express their gratitude to the Beatson radiotherapy and diagnostic radiography staff.

References

1. Khoo VS. MRI—''Magic radiotherapy imaging'' for treatment planning? Br J Radiol 2000;73:229–33.
2. Charnley N, Morgan A, Thomas E, Wilson S, Bacon S, Wilson D, et al. The use of CT-MR image registration to define target volumes in pelvic radiotherapy in the presence of bilateral hip replacements. Br J Radiol 2005;78:634–6.
3. Sannazzari GL, Ragona R, Ruo Redda MG, Giglioli FR, Isolato G, Guarneri A. CT–MRI image fusion for delineation of volumes in three-dimensional conformal radiation therapy in the treatment of localized prostate cancer. Br J Radiol 2002;75:603–7.
4. Sefrova J, Odrazka K, Paluska P, Belobradek Z, Brodak M, Dolezel M, et al. Magnetic resonance imaging in post-prostatectomy radiotherapy planning. Int J Radiat Oncol Biol Phys 2012;82:911–18.
5. Khoo VS, Joon DL. New developments in MRI for target volume delineation in radiotherapy. Br J Radiol 2006;79: S2–S15.
6. Smith WL, Lewis C, Bauman G, Rodrigues G, D'Souza D, Ash R, et al. Prostate volume contouring: A 3D analysis of segmentation using 3DTRUS, CT, and MR. Int J Radiat Oncol Biol Phys 2007;67:1238–47.
7. Rasch C, Barillot I, Remeijer P, Touw A, van Herk M, Lebesque JV Definition of the prostate in CT and MRI: A multi-observer study. Int J Radiat Oncol Biol Phys 1999;43:57–66.
8. Chung NN, Ting LL, Hsu WC, Lui LT, Wang PM. Impact of magnetic resonance imaging versus CT on nasopharyngeal carcinoma: primary tumor target delineation for radiotherapy. Head Neck 2004;26:241–6.
9. Ahmed M, Schmidt M, Sohaib A, Kong C, Burke K, Richardson C, et al. The value of magnetic resonance imaging in target volume delineation of base of tongue tumours—a study using flexible surface coils. Radiother Oncol 2010;94:161–7.
10. Rosenman JG, Miller EP, Tracton G, Cullip TJ. Image registration: an essential part of radiation therapy planning. Int J Radiat Oncol Biol Phys 1998;40:197–205.
11. Geets X, Daisne JF, Arcangeli S, Coche E, De Poel M, Duprez T, et al. Inter-observer variability in the delineation of pharyngo-laryngeal tumor, parotid glands and cervical spinal cord: comparison between CT-scan and MRI. Radiother Oncol 2005;77:25–31.
12. Khoo VS, Adams EJ, Saran F, Bedford JL, Perks JR, Warrington AP, et al. A comparison of clinical target volumes determined by CT and MRI for the radiotherapy planning of base of skull meningiomas. Int J Radiat Oncol Biol Phys 2000;46:1309–17.
13. Prabhakara R, Haresh KP, Ganesh T, Joshi RC, Julka PK, Rath GK. Comparison of computed tomography and magnetic resonance based target volume in brain tumors, J Canc Res Ther 2007;3:121–3.
14. Doran SJ, Charles-Edwards L, Reinsberg SA, Leach MO. A complete distortion correction for MR images: I. Gradient warp correction. Phys Med Biol 2005;50:1343–61.

15. Fransson A, Andreo P, Pötter R. Aspects of MR Image Distortions in Radiotherapy Treatment Planning. Strahlenther Onkol 2001;177:59–73.
16. Schenck JF. The role of magnetic susceptibility in magnetic resonance imaging: MRI magnetic compatibility of the first and second kinds. Med Phys 1996;23:815–50.
17. Moore CS, Liney GP, Beavis AW. Quality assurance of registration of CT and MRI datasets for treatment planning of radiotherapy for head and neck cancers. J Appl Clin Med Phys 2004;5:25–35.
18. Veninga T, Huisman H, Maazen RWM, Huizenfa H. Clinical validation of the normalised mutual information method for registration of CT and MR images in radiotherapy of brain tumors. J Appl Clin Med Phys 2004;5: 66–79.
19. Mutic S, Dempsey JF, Bosch WR, Low DA, Drzymala RE, Chao KS, et al. Multimodality image registration quality assurance for conformal three-dimensional treatment planning. Int J Radiat Oncol Biol Phys 2001;51:255–60.
20. Li G, Xie H, Ning H, Citrin D, Capala J, Maass-Moreno R, et al. Accuracy of 3D volumetric image registration based on CT, MR and PET/CT phantom experiments. J Appl Clin Med Phys 2008;9:17–36.
21. Institute of Physics in Engineering and Medicine. Report 80 quality control in magnetic resonance imaging. York, UK: IPEM; 1998.
22. American Association of Physicists in Medicine. Acceptance testing and quality assurance procedures for magnetic resonance imaging facilities. College Park, MD: AAPM; 2010.
23. McJury M, O'Neill A, Lawson M, McGrath C, Grey A, Page W, et al. Assessing the image quality of pelvic MR images acquired with a flat couch for radiotherapy treatment planning. Br J Radiol 2011;84:750–5.
24. Zou KH, Warfield SK, Bharatha A, Tempany CM, Kaus MR, Haker SJ, et al. Statistical validation of image segmentation quality based on a spatial overlap index. Acad Radiol 2004;11:178–89.
25. Dearnaley D, Syndikus I, Sumo G, Bidmead M, Bloomfield D, Clark C, et al. Conventional versus hypofractionated high-dose intensity-modulated radiotherapy for prostate cancer: preliminary safety results from the CHHiP randomised controlled trial. Lancet Oncol 2012;13:43–54.
26. Reit A, Mak ACA, Moerland MA, Elders LH, Zee W. A conformation number to quantify the degree of conformality in brachytherapy and external beam irradiation: application to the prostate. Int J Radiat Oncol Biol Phys 1997;37:731–6.